Seminar series nr 159

Potential of a Post-Classification Change Detection Analysis to Identify Land Use and Land Cover Changes.

A Case Study in Northern Greece

Florian Sallaba

2009
Geobiosphere Science Centre
Physical Geography and Ecosystems Analysis
Lund University
Sölvegatan 12
223 62 Lund
Sweden

Potential of a Post-Classification Change Detection Analysis to Identify Land Use and Land Cover Changes.

A Case Study In Northern Greece.

Florian Sallaba

Bachelor's Degree in Physical Geography and Ecosystem Analysis

Supervisor:

Ulf Helldén

Department of Physical Geography and Ecosystem Analysis

Lund University

Abstract

The use of remotely sensed data is an important method to indicate land use and land cover changes. Remote sensing can provide a better picture of monitoring land use and land cover changes. It makes it feasible to locate geographically changed areas in order to employ it further detailed studies on environmental changes (e.g. land degradation).

The study area is a heterogeneous and small-structured agriculturally dominated prefecture in northern Greece.

The core post-classification change detection analysis was based on two Landsat 5 TM and Landsat 7 ETM+ images. **Maximum likelihood classification** was applied on the satellite data. A basic arithmetic combination was used to compare the classification outcomes to detect and locate land use and land cover changes over a period of 14 years. The accomplished post-classification change detection analysis performed weakly.

Key words: Physical Geography, Geography, Change Detection, Maximum likelihood classification, Remote Sensing, Land Use Land Cover, Greece, Imathia

Sammanfattning

Användandet av fjärranalysdata är en viktig metod för att bestämma markanvändning och visa på förändringar i marktäcke. Fjärranalys kan ge en bättre utgångspunkt för övervakning av markytstäcke. Det gör det möjligt att geografiskt lokalisera förändrade markområden för att vidare kunna utföra noggrannare undersökningar om miljöförändringar (t.ex. markdegradering).

Studieområdet är ett administrativt distrikt i norra Grekland. Det är ett heterogent jordbruksdominerat område karakteriserat av småskaliga landskapsstrukturer.

Markförändringsanalysen efter klassifikation baserades på två bilder från Landsat 5TM och Landsat 7 ETM+. **Maximum likelihood classification** användes för klassifikation av satellitdatan. En kombination av enkel aritmetisk matematik användes för att jämföra resultatet av klassifikationerna och lokalisera förändringar i markanvändning och markytstäcke över en period på 14 år. Den utförda markförändringsanalysen fungerade inte väl.

Nyckelord: Naturgeografie, Geografie, Change Detection, Maximum likelihood classification, Fjärranalys, Markanvändning och markytstäckning, Grekland, Imathia

Index of Contents

Abstract *5*

Sammanfattning *5*

1. Introduction *9*

2. Objectives *10*

3. Study Area *10*

4. Methods and Data *12*

4.1 Data **12**
4.1.1 Data Acquisition 12
4.1.2 Sensor Characteristics 12

4.2 Pre – processing **14**
4.2.1 Geometric Processing 14
4.2.2 Radiometric Calibration 14
4.2.3 Image Enhancement 17

4.3 Supervised Classification **21**
4.3.1 Information Classes 21
4.3.2 Spectral Signature Classes 21
4.3.3 Maximum Likelihood Classification 22
4.3.4 Map Accuracy Assessment 23
4.3.5 Post Classification Processing 25

4.4 Change Detection **25**

5. Results..... 27

5.1 Maximum Likelihood Classification 27

5.2 Post-classification Change Detection..... 28

6. Discussion..... 31

7. Conclusion 37

8. Literature..... 38

Appendix Figures 42

Appendix Maps I..... 43

Appendix Maps II..... 44

Appendix Maps III..... 45

Appendix Maps IV 46

Index of Figures

Figure 1 *Climate Data Of Trikala Obtained From Hellenic National Meteorological Service (2008)* 11
Figure 2 *Comparison Of TM Bands And Selected Spectral Signatures (Baldridge, 2009)* 17
Figure 3 *Orthogonal Rotation Of Axes Via PCA* 18
Figure 4 *Post-Classification Change Detection Scheme* 26
Figure 5 *Land Cover Distribution Of Imathia Obtained Via Classification* 28
Figure 6 *Areal Gain And Loss Of Generalised LULC Change Classes* 30
Figure 7 *Distribution Of Main Crops in Central Macedonia (Albanis et al. 1998)* 42
Figure 8 *Fictional LULC Change Development* 42

Index of Tables

Table 1 *Landsat TM And ETM+ Specifications On The Basis Of Kramer (2001) And Lillesand et al. (2000)* 13
Table 2 *Postcalibration Dynamic Ranges for NLAPS Data (Chander and Markham 2003 and, NASA, 1999) Spectral Radiance, Lminλ and Lmaxλ in W/(m²*sr*μm) and Solar Spectral Irradiance, Esunl, in W/(m²*μm)* 15
Table 3 *Sun Elevation, Earth-Sun Distance And Solar Zenith Angles* 16
Table 4 *Detailed Change of Detected LULC Classes* 30

Index of Equations

Equation 1 *Conversion To Spectral Radiance From Chander and Markham (2003):* 15
Equation 2 *Earth-Sun-distance From Seaquist (NGEN08 Course Materials, Lund University, 2008)* 16
Equation 3 *Spectral Radiance To T-O-A Reflectance Chander and Markham (2003)* 16
Equation 4 *Weighted Difference Vegetation Index From Eastman (2006)* 20
Equation 5 *Kappa Coefficient From Lillesand et al. (2000)* 24

1. Introduction

This bachelor thesis is written for taking exam in the bachelor program of Physical Geography and Ecosystem Analysis at the University of Lund. It deals with a land use and land cover (LULC) change study in northern Greece.
I am grateful for the supervision of Professor Ulf Helldén, Department of Physical Geography and Ecosystem Analysis, Lund University, Sweden.

The monitoring of LULC changes has become a major environmental research issue in scientific, political and popular discussions over the last decades. LULC changes are feasible to identify direct and indirect land degradation processes. The monitoring of LULC changes has been supported in several projects by governments and international organisation such as European Union and United Nations Organisation.
The United Nations Conference on Environment and Development (1992) defines desertification as land degradation in arid, semi-arid and dry sub-humid areas resulting from various causes, including climatic variations and human activities.

The chosen study area is a heterogeneous agricultural region in northern Greece. Its physical settings equates to the definition of Salvati and Zitti (2008) for areas that are potentially affected by land degradation processes. Therefore a monitoring of LULC changes is practicable.

Remote sensing contributes to a better understanding of LULC changes. Consequently, a specific mathematical pixel-by-pixel pattern recognition algorithm is tested on Landsat 5 TM and Landsat 7 ETM+ satellite data with the intention of classifying LULC in the study site. Pixel-by-pixel based classification algorithms were well applied to detect LULC in other study areas in Greece (Symeonakis et al., 2004 and Vasilakos et al., 2004).
Eastman (2006) suggests the use of satellite imagery as an important input for land use and land cover change studies. It has the capability to provide timely and historical information that may be impossible to obtain in any other way.

2. Objectives

The purpose of this thesis is to study the potential of a post-classification change detection analysis using remotely sensed data in order to identify changes of LULC in the prefecture of Imathia, northern Greece. This post-classification change detection approach will be based on maximum likelihood classification algorithm using Landsat 5 TM and Landsat 7 ETM+ satellite data. The results will represent a qualitative measurement of LULC classes of two points in time.

These qualitative data will be applied for a post-classification change detection analysis over a period of 14 years to quantify the spatial extent of each LULC change class.

A change detection map will be produced with the intention of locating LULC change classes geographically. In addition, LULC change classes will be inspected for their informational value in order to figure out if a LULC change class makes sense.

3. Study Area

The case study area of Imathia is a prefecture situated in the periphery of Central Macedonia and its capital is Veria. Imathia covers an area of 1701 km^2, has a total population of 144 354 and a population density of 85 per km^2. Its geography consists mainly of the Central Macedonian lowland, which is abundant with water and mountainous parts of Pierian Mountains to the southeast as well as the Verminion Mountains to the west. It has a small coast of the Thermaikos Gulf. An overview map of Imathia is provided in Appendix Map I.

The climate is classified as semi-arid to sub-humid with hot summers and cold wet winters. Figure 1 illustrates the monthly average precipitation and temperature at the climate station of Trikala (22° 33' 12"E/40° 15' 43"N) in the study area over the period of 1980 to 1997. Maximum precipitation takes place in spring and autumn, although strong precipitation events might happen in other periods. Trikala has an average annual precipitation of 506mm. The highest temperatures occur in July (26 °C) and the lowest in January (5°C). The driest and warmest conditions take place between May and September.

Karyotis et al (2006) reveal that 88.2% of the soils belong to the order of Entisols, whereas the rest are of Inceptisols in the lowland of Imathia. Vegetation types are usually

agricultural crops in the lowland. Main irrigated perennial crops in Imathia are peach (Prunus persica), pear (Pirus communis) and apple trees (Pirus malus).

The dominant annual crops in the study area are cotton (Gossypium hirsutum L.), corn (Zea mays L.), sugar beet (Beta vulgaris L.) and rainfed winter wheat (Triticum aestivum L.). About 82% of irrigation demands in the lowlands are covered by surface water via a dense collective network, the remaining 18% are supplied from groundwater (Karyotis et al.2006). Aliakmon river and the small rivers Tripotamos and Arapitsa form the main irrigation sources for the lowland of Imathia (Albanis et al. 1996).

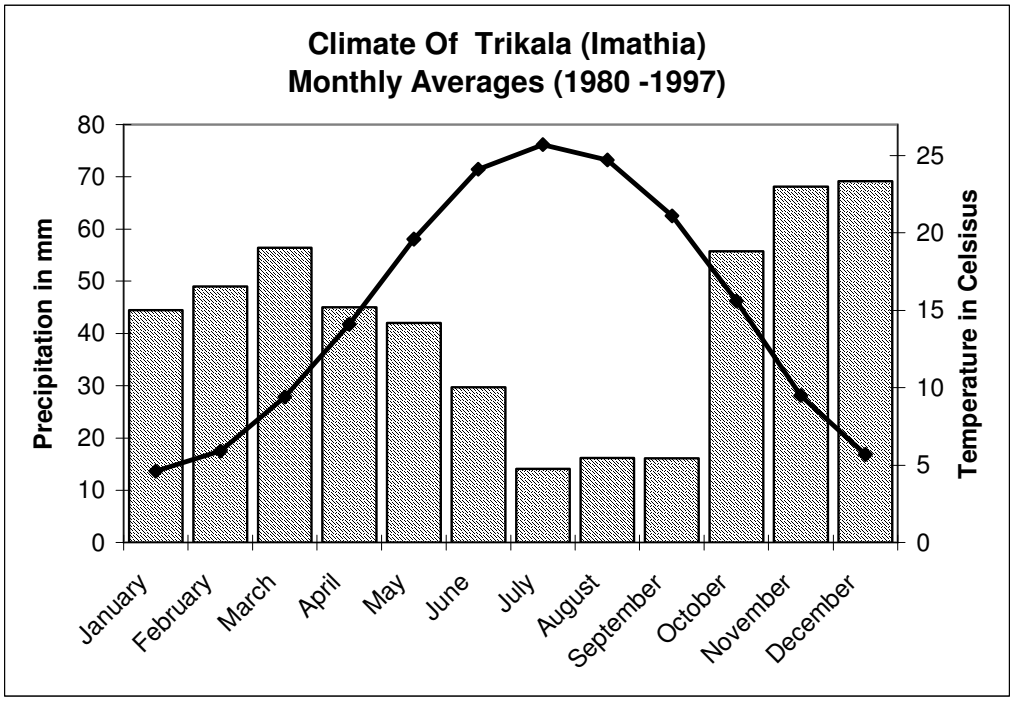

Figure 1 Climate Data Of Trikala Obtained From Hellenic National Meteorological Service (2008)

The rural economy of Imathia is strongly dependent on agricultural production and export of fruits such as peaches and grapes. Additional income sources are the industry sector that is related to agriculture (food industry), tourism and livestock grazing in mountainous rangeland areas. Intensive agriculture is practised and most crops are irrigated. In figure 7 (see Appendix Figures) is shown Central Macedonia's distribution of major crops based on Albanis et al. (1998).

4. Methods and Data

4.1 Data

4.1.1 Data Acquisition

It is essential for a change detection to choose appropriate calendar acquisition dates and temporal resolutions. Anniversary dates of satellite images have the capability to minimise discrepancies in reflectance caused by seasonal vegetation fluxes and Sun angle differences. Anniversary dates are recommended for bi-temporal change detection. On the other hand, on anniversary dates as well phenological disparities due to local precipitation and temperature variations can appear (Coppin et al., 2004). One should consider common seasonal varieties in beginning and end of a season.

As satellite data provider was used the Global Land Cover Facility (GLCF) of the University of Maryland and distributes remotely sensed data exempt from charges. A Landsat 5 Thematic Mapper (TM) recorded in summer 1987 (19/07/1987) and a Landsat 7 Enhanced Thematic Mapper Plus (ETM+) gathered in late spring 2001 (30/05/2001) were selected.

Furthermore, digital data of Greece provided by ESRI® Data & Maps (2008) in order to process in a Geographical Information System (GIS) was utilised.

4.1.2 Sensor Characteristics

Landsat 5 TM was launched on 5th March 1985 into repetitive, circular, sun – synchronous and near polar orbit. These orbits have an inclination angle of 98.2° with respect to the equator and an orbital altitude of 705km. It is a swath width of 185km for imaging used. This spacecraft crosses the equator on the north – to – south portion of each orbit at 9:45 A.M. local sun time. Each orbit takes approximately 99 min, with over 14.5 orbits being completed in a day and results in a 16 – day repeat coverage (Lillesand et al. 2000). It has the Thematic Mapper (TM) on board, which is a multi-spectral mechanically scanning optical imager operating in the visible and infrared ranges.
The spectral and spatial ground resolution of TM can be found in table 1 (TM bands are superscripted with [a]).

Table 1 Landsat TM And ETM+ Specifications On The Basis Of Kramer (2001) And Lillesand et al. (2000)

Band no.	Wavelength (μm)	Spectral light	Pixel/ Ground resolution (m)	Principal Applications
1	0.45 – 0.52	Blue	30	Distinction of soil, water and vegetation
2 [a]	0.52 – 0.60	Green	30	Distinction of vegetation
2 [b]	0.53 – 0.61			
3	0.63 – 0.69	Red	30	Distinction of vegetation and soils
4[a]	0.76 – 0.90	Near infrared	30	Biomass and urban areas
4[b]	0.78 – 0.90			
5[a]	1.55 – 1.75	Shortwave infrared	30	Distinction of vegetation and rocks
5[b]	1.55- 1.78			
6[a]	10.40 – 12.50	Thermal infrared	120	Measuring of temperature
6[b]	10.42 – 11.66		60	
7[a]	2.08 – 2.35	Shortwave infrared	30	Amount of water in vegetation and soils
7[b]	2.10 – 2.35			
8 [b]	0.50 – 0.90	Panchromatic	15	Distinction of areas

[a]Band specifications of Landsat 5 TM and [b]Band specifications of Landsat 7 ETM+

Landsat 7 ETM+ was launched on the 15th April 1999. The earth – observing instrument onboard this spacecraft is the Enhanced Thematic Mapper Plus (ETM+), which is a fixed across-track radiometer (Kramer 2001). The design of the ETM+ stresses the provision of data continuity with Landsat 5. Similar orbits and repeat patterns are used, as is the 185km swath width for imaging (Lillesand et al. 2000). Enhancements are the addition of a 15m-ground resolution panchromatic band and an improved thermal band with 60m- ground resolution. The spectral and spatial ground resolutions of ETM+ are illustrated in table 2 (ETM+ bands are superscripted with [b]).

A more detailed description of the spacecrafts and their sensors characteristics is available in the Landsat 5 and 7 Science Data Users Handbooks (NOAA 1984 and NASA 1999) and Kramer (2001).

These similar sensor specifications of Landsat TM and ETM+ allow a meaningful comparison of the data sets.

4.2 Pre – processing

4.2.1 Geometric Processing

Pre-processing of satellite sensor images is necessary in order to establish more direct linkage between the data and biophysical phenomena, removal of data acquisition errors, image noise and masking of contaminated and irrelevant spots such as clouds or water bodies, which might lead to misinterpretation and detection of unreal change phenomena (Coppin et al., 2004). The satellite data was clipped to a subset of the case study area in order to focus on the relevant data. Cloud coverage was masked out in both subsets to exclude contaminated pixels. Approximately 3030 ha (2%) of satellite data was masked out.

Landsat imagery provided by the GLCF include a UTM projection and a WGS84 datum and ellipsoid respectively. Thus a geometric correction was unnecessary. However the vector data in the GIS needed to be projected to the Landsat imagery UTM projection, WGS84 datum and ellipsoid.

4.2.2 Radiometric Calibration

It is important to calibrate raw sensor data to meaningful physical units prior to a post-classification change detection. A radiometric calibration helps to be sure that detected changes can be taken for real instead of errors caused by differences in sensor calibration and Sun angles. Unreal change phenomena could be caused by temporal variations in the solar zenith and azimuth angles (Coppin et al. 2004). The radiometric calibration in this study includes a conversion from calibrated digital numbers to spectral radiance and a spectral radiance to top-of-atmosphere (TOA) reflectance as recommended by Chander and Markham (2003). A full atmospheric correction was not performed. This is recommended by Song et al. (2001), they described the very small effect of an atmospheric correction for a post-classification change detection accuracy. Each image should be classified individually with different signature training data on the same scale (see Chapter 4.3 – Supervised Classification) and then compared to monitor changes.

Spectral Radiance

The calculation of spectral radiance in W/(m²*sr*μm) is used to place different imagery into a common radiometric scale and to take sensor related effects into account (Chander et al., 2003 and Pilesjö, 1992). A conversion from quantized calibrated pixel values to spectral radiance (L_λ) was accomplished trough Equation 1 (Chander and Markham 2003).

Equation 1 *Conversion To Spectral Radiance From Chander and Markham (2003):*

$$L_\lambda = \left(\frac{LMAX_\lambda - LMIN_\lambda}{Q_{cal\max}} \right) * Q_{cal} + LMIN_\lambda$$

Where:

L_λ	*Spectral radiance at the sensor' s aperture in W/(m²*sr*μm);*
Q_{cal}	*Quantized calibrated pixel value in Digital Numbers (DNs);*
Q_{calmin}	*Minimum quantized calibrated pixel value (DN = 0) corresponding to $LMIN_\lambda$;*
Q_{calmax}	*Maximum quantized calibrated pixel value (DN = 255) corresponding to $LMAX_\lambda$;*
$LMIN_\lambda$	*Spectral radiance that is scaled to Qcalmin in W/(m²*sr*μm);*
$LMAX_\lambda$	*Spectral radiance that is scaled to Qcalmax in W/(m²*sr*μm).*

The used parameters of the corresponding sensor are illustrated in table 4 post-calibration dynamic ranges for National Landsat Archive Production System (NLAPS) Data (Chander and Markham 2003 and Landsat 7 ETM+ Sciene Data Users Handbook (NASA), 1999).

Table 2 *Postcalibration Dynamic Ranges for NLAPS Data (Chander and Markham 2003 and, NASA, 1999) Spectral Radiance, Lminλ and Lmaxλ in W/(m²*sr*μm) and Solar Spectral Irradiance, Esunl, in W/(m²*μm)*

Band	Landsat 7 ETM+			Landsat 5 TM		
	$Lmin_\lambda$	$Lmax_\lambda$	$Esun_l$	$Lmin_\lambda$	$Lmax_\lambda$	$Esun_l$
1	-6.20	191.60	1969.00	-1.52	152.10	1957
2	-6.40	196.50	1840.00	-2.84	296.81	1826
3	-5.00	152.90	1551.00	-1.17	204.30	1554
4	-5.10	241.10	1044.00	-1.51	206.20	1036
5	-1.00	31.06	225.70	-0.37	27.19	215
6	0	17.04	N/A	1.2378	15.303	N/A
7	-0.35	10.80	82.07	-0.15	14.38	80.67
8	-4.70	243.10	1368.00	none	none	none

Top Of Atmosphere Reflectance

Different sun angles and solar irradiance were normalised by calculating the TOA reflectance in unitless planetary reflectance. This computation was done with Equation 3 according to Chander and Markham (2003). It needs the Earth-Sun distance in astronomical units and the Solar zenith angle. In table 3 one can see these parameters, which were computed with Equation 2 in Appendix Equations. Chander and Markham (2003) recommend these calculations as a reduction in between-scene variability, because the cosine effect of different solar zenith angles can be removed. On the other hand one should consider that it does not add new information to the image.

Equation 2 *Earth-Sun-distance From Seaquist (NGEN08 Course Materials, Lund University, 2008)*

$$d = 1 + 0.0167 * \sin\left(2\pi\left(Julianday - 93.5\right)/365\right)$$

where:

d *Earth-sun distance in astronomical units.*

Equation 3 *Spectral Radiance To T-O-A Reflectance Chander and Markham (2003):*

$$\rho_{\mathrm{P}} = \frac{\Pi * L_{\lambda} * d^{2}}{ESUN_{\lambda} * \cos\theta_{s}}$$

Where:

ρ_P *Unitless planetary reflectance;*

L_λ *Spectral radiance at the sensor' s aperture in W/(m²*sr*μm);*

d *Earth-sun distance in astronomical units;*

$ESUN_\lambda$ *Mean solar exoatmospheric irradiances in W/(m²*μm);*

θ_s *Solar zenith angle in degrees*

Table 3 *Sun Elevation, Earth-Sun Distance And Solar Zenith Angles*

Satellite Scene of Imathia	Sun elevation in degrees	Earth-sun distance in astronomical units	Solar zenith angle in degrees	Solar zenith angle in radians
Landsat 5 TM	57	1.01613	33	0.57596
Landsat 7 ETM+	63.76	1.00258	26.24	0.45797

4.2.3 Image Enhancement

Image enhancement is valuable to detect and define LULC information classes since they have different spectral characteristics. A proper image enhancement includes multi-spectral transformation, false colour composites and vegetation indices, which is important to achieve information of the area and spectral knowledge.

Reflectance Characteristics

Surfaces have different reflectance characteristics over the electromagnetic radiation spectrum as one can see in the figure 2, which is based on Baldridge et al. (2009), data of the Aster Spectral Library Version 2.0 provided by California Institute of Technology. In figure 2 are illustrated three occurring surfaces in Imathia and how they can be approximately detected within the Landsat 5 TM sensor system. Vegetation has its characteristic spectral signature with the green peak in visible green light, a decrease in the visible red light and a strong boost in the near infrared called red edge. The spectral signature of soil such as Entisol has a slight increase in the visible light, a short strong increase in the near infrared and then a slight increase in the whole infrared. Man-made surfaces such as asphalt have an almost constant spectral signature on a low reflectance level over the electromagnetic radiation spectrum.

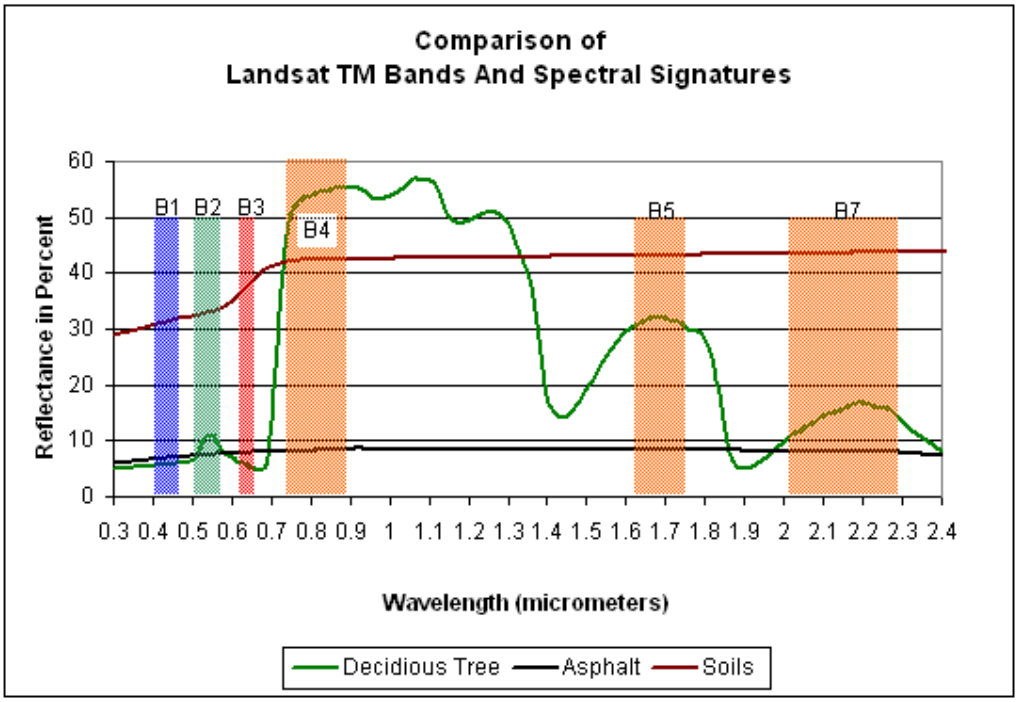

Figure 2 Comparison Of TM Bands And Selected Spectral Signatures (Baldridge, 2009)

Principal Component Analysis

A multi-spectral transformation is a common application by reason of inter-band-correlation in multi-spectral image data. Moreover Fung and LeDrew (1987) mention that multi-spectral remote sensing data exhibit high inter-band-correlation. That means if reflectance are high at a particular spot in one band this spots are likely to be high in other bands. Multi-spectral transformation allow to generate new and fewer sets of image components. The outcome is an alternative description of the original data and new components are uncorrelated. In addition they carry new information and are ordered in terms of the amount of image variation they can explain (Eastman, 2006). In brief information is maximized in the first component and decrease successively in the following. In this study a principal component analysis (PCA) was performed.

Mathematically a linear transformation was applied that defines new orthogonal components with their origin at the mean of the data distribution as one can see in figure 3. This transformation describes linear combinations of the original data values multiplied by appropriate transformation coefficients, called eigenvectors. Eigenvectors, a statistical quantity, are derived from the variance or covariance matrix of the original data (Lillesand et al., 2000).

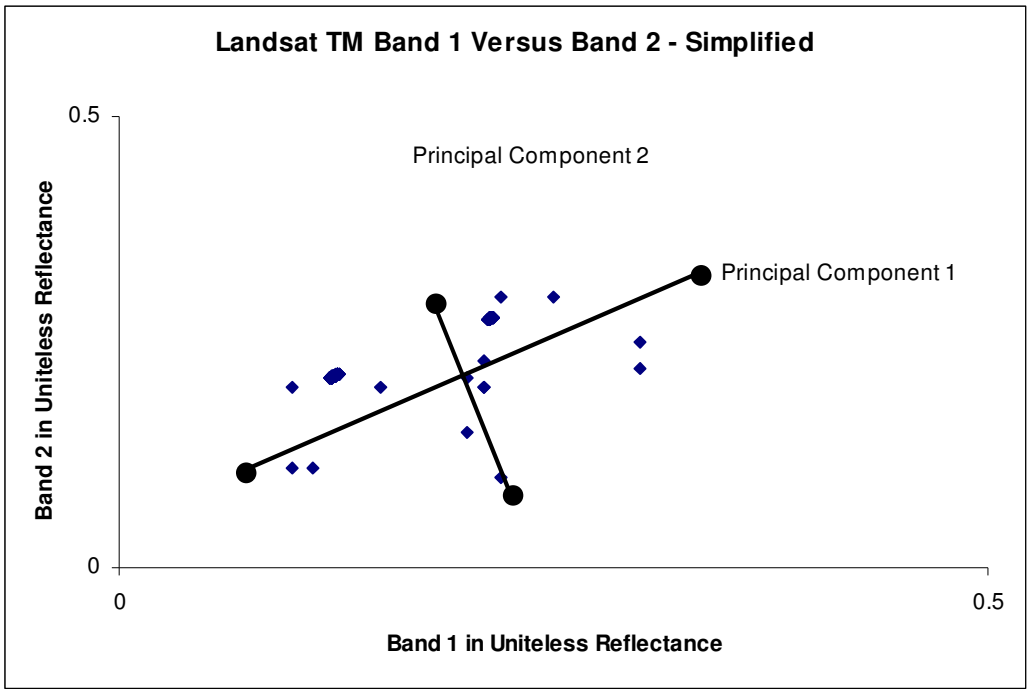

Figure 3 Orthogonal Rotation Of Axes Via PCA

However the new components of a pixel vector are related to its old DN in the original set of spectral bands. PCA is recommended by Lillesand et al. (2000) for scenes where little prior knowledge is available and to optimise the implementation of maximum likelihood classification. Kuemerle et al. (2006[b]) employed successfully PCA to enhance TM and ETM+ data in a classification approach. More detailed descriptions of PCA and its statistical terms can be found in remote sensing literature (Lillesand et al. 2000; Richards and Jia, 1998 and Eastman; 2006).

Weighted Difference Vegetation Index

A more simple multi-spectral transformation is the utilisation of vegetation indices (VI's). Advantages of VI's over single band radiometric responses are their capability to provide information not available in any single band (Coppin et al. 2004) and their possibility to reduce data (Richards and Jia, 1999). For each environment adequate indices can be applied. In the semi-arid environment of Imathia was a distance based vegetation index accomplished in order to detect appropriate training areas and to achieve knowledge of the area.

According to Eastman (2006) distance based vegetation indices are appropriate for average reflectance, which are influenced by soil background. They help to take apart information about vegetation from information about soil. Distance based vegetation indices apply the concept of a soil line and distances from it. A soil line is a linear regression that describes the relationship between reflectance values in the red and near infrared bands for **bare soil pixel**. Bare soil pixels were digitised in both Landsat images. All pixels in the data that have the same reflectance relationship are assumed to be bare soils. Those, which are located far from the soil line are supposed to be vegetation or water (Eastman, 2006).

Of interest in the study area are unknown pixels that have higher reflectance in the near infrared and are assumed to be vegetation (compare figure 2).

A weighted difference vegetation index (WDVI) was applied in order to maximise the vegetation signal in the near infrared band and to minimise soil brightness. Equation 4 describes the WDVI calculation (Eastman, 2006).

Thus vegetation was enhanced and linked to the iterative spectral signature improvement procedure.

Equation 4 *Weighted Difference Vegetation Index From Eastman (2006)*

$$WDVI = \rho_n - \gamma * \rho_r$$

Where:

ρ_n	*Reflectance of near infrared band*
ρ_r	*Reflectance of visible red band*
γ	*slope of the soil line*

False Colour Composite

A full colour image is based on the Red Green Blue system (RGB), which is an additive colour mixing. The RGB system allows using three corresponding colour guns that display available satellite spectral bands. This offers a possibility to combine bands and colour guns in a different way in order to enhance the image.

For a true colour composite one uses the red colour gun for spectral bands in the visible red light, green colour gun for spectral bands within the visible green light and the blue colour gun for spectral bands in the visible blue light. For false colour composites (FCC) one can use each available satellite spectral band. It is common to include several spectral bands that are more targeted to a differentiation of specific surface materials according to Eastman (2006).

FCC's and an associated contrast stretching (compare Lillesand et al., 2000 and Richards and Jia, 1999) of both images were carried out. This method is recommended by Eastman (2006) as a useful tool of image enhancement for the reason that it allows a simultaneous visualisation of information from three separate spectral bands as well as information that are not visible to the human eye in the infrared wavelengths.

By dint of TM sensor characteristics (compare figure 2 and table 1 above) and reflectance characteristics two FCC's were used to detect surfaces in this study area.

The first FCC has band 7 in the red colour gun, band 4 in the green colour gun and band 3 in the blue colour gun (FCC R:7, G:4 and B:3). This composite is useful to distinguish between soil and urban areas because soils appear in a smooth rose colour whereas urban surfaces appear in blue violet colour. Thus it is practical in study area of Imathia.

The second is a classic infrared FCC which is used to detect vegetation because it has band 4 in the red colour gun, band 3 in the green colour gun and band 2 in the blue colour gun (FCC is R:4, G:3 and B:2). Vegetated surfaces are displayed in reddish colours.

4.3 Supervised Classification

4.3.1 Information Classes

The achievement of sufficient spectral signatures is based on user digitised training sites and their corresponding information classes. In case of this study a determination of information classes needs to take knowledge of the area and seasonal independence into account.

A good knowledge of the study area was achieved by a suitable image enhancement and literature studies. Furthermore Richards and Jia (1999) suggest fieldwork that develops knowledge of the area with interviews, photography of characteristic surfaces, spectral measurements and collecting of ground truth data in order to validate a classification. Fieldwork was not carried out. Seasonal independence of information classes means that classes should be free of seasonal variations because the satellite data were not recorded on an anniversary date. This might be the main error source at the later change detection analysis. The information classes are chosen by the help of the USGS land use and cover classification system recommended by Lillesand et al. (2000). The information classes are agriculture, forest, soil, water and urban. Agriculture is divided in sub classes to consider the different spectral signatures of cropland and arable-land as well as the seasonal differences in both images.

The class soil includes bedrocks and sparse vegetated areas since soil signatures dominate the background signals in the Mediterranean basin and lead to confusion. Compare subsection 4.3.2 – Spectral Signature Classes as well as Hostert et al. (2003) and Röder et al. (2008). Rangelands were not taken into account for the reason that they are quite difficult to identify in the satellite images without fieldwork and reference data such as topographic maps and air photography. However, sparse vegetation and ruderal species that could be used for grazing are assumed to be in the soil class due to the dominating soil background signal.

4.3.2 Spectral Signature Classes

Creating spectral signature classes is an iterative process and its objective is to aggregate a set of statistical data that describe the spectral signature of each information class. For a MLC training statistics of spectral classes consist of their mean vectors and their covariance matrices (Richards and Jia, 1999).

Common image processing systems offer possibilities such as scatterplots to enhance those signatures. Scatterplots are two dimensional multi-spectral feature spaces with defined axes. In order to create satisfactory spectral signatures of each information class and subclass respectively an adequate amount of training sites were digitised in both satellite images. Lillesand et al. (2000) describe the determination of training sites as art and science, since it needs a close interaction between user and the image as well as adequate reference data. In addition the mixed pixel problem of TM and ETM+ data was considered. The ground resolution of 30m leads to a mixture of several spectral signatures in a pixel. Lillesand et al (2000) mention this problem of sensors to record and extract spatial and spectral detail in an image. Therefore training sites of the corresponding information class were made in explicit areas in order to be representative and complete, whereas the soil class is an exception as mentioned above. The spectral signature class statistics were estimated in both Landsat images out of the bands 3,4,5 and 7 as well as the principal components 1 and 2. Richards and Jia (1999) recommend this kind of selection if bands or features do not support discrimination significantly.
Band 6 was excluded due to the inconsistency in the spatial resolution (Ediriwickrema and Khorram, 1997).

4.3.3 Maximum Likelihood Classification

Although many different methods have been devised to implement supervised classification, the MLC is still one of the most widely used supervised classification algorithms (Jensen, 1996). In this study a MLC algorithm was employed. It quantitatively evaluates the variance and covariance of the spectral response patterns of an unknown pixel (Lillesand et al., 2000). The algorithm is able to recognise the spectral characteristics of each class in an unknown data set via the statistical data obtained by digitised training sites beforehand (Richards and Jia, 1999). It assumes a multivariate normal distribution of each spectral class. The mean vector and covariance matrix of a distribution can be used to describe it completely. By dint of these parameters it is possible to estimate a statistical probability of a given pixel value being a member of a particular spectral class. The outcome is a probability density function for each spectral class. These probability density functions are employed to assign an unidentified pixel by computing the probability of the pixel value belonging to each spectral class. In the end a pixel would be assigned to the most likely spectral class or be assigned as unclassified if the probability values are below a user defined threshold (Lillesand et al., 2000).

In brief it is an estimation of a class membership of an unknown pixel using multivariate normal distribution models for the classes. A MLC algorithm can model class distributions that are lengthened to different extents in different directions in the multi-spectral feature space and leads to minimum average classification error if it is applied properly.

On the other hand MLC is sensitive to the assumption of multivariate normal distribution. The spectral classes should be single distributions and often the classes are multimodal (Richards and Jia, 1999). Therefore the iterative step of determining spectral class signatures was repeated by dint of scatterplots to avoid multimodal training data. However, some spectral classes naturally have these characteristics and overlaps such as soil, arable-land and urban areas. A more detailed statistical explanation of the MLC algorithms and its statistical terms are described in Richards and Jia (1999) and Lillesand et al. (2000).
The outcomes of the MLC were two thematic maps of Imathia in 1987 and 2001 according to the spectral classes (cropland, arable-land, forest, soil, water and urban).

4.3.4 Map Accuracy Assessment

A map accuracy assessment should always follow a classification in order to test the quality of the classification. Different authors suggest such an accuracy assessment. It needs ground truth data of the corresponding study area. This data are preferably sample points measured with a Global Positioning System (GPS) device with information about the dominating LULC class at this point. In addition one should consider the ground resolution of the sensor system by describing the prevailing LULC type. Satisfactory ground truth data should be collected ideally in the same week where the satellite image was recorded.

An assessment of this study would need ground truth data for both Imathia maps collected in 1987 and 2001. Ground truth points should be randomly distributed sample points over the study area. Each spectral class should be represented by at least 15 sample points. A map accuracy assessment is used to employ an error matrix, which shows the frequency of pixels in each category. Out of an error matrix user accuracy and producer accuracy should be estimated.

The user accuracy is calculated from number of correct sample points in a class divided by number of sample of that class in the map. It illustrates the probability of an unknown point on the map of being correctly mapped.

The producer accuracy is estimated from number of correct sample points in a class divided by number of points of that class in the ground truth data. It describes the probability of an unknown point in the field as well as of being correctly mapped.

Furthermore the Kappa coefficient, see Equation 5, should be computed to explain proportional improvement of the classification over a random assignment of classes. A detailed explanation of map accuracy assessment can be found in Richards and Jia (1999) and Lillesand et al. (2000).

Equation 5 *Kappa Coefficient From Lillesand et al. (2000)*

Kappa Coefficient:

$$\kappa = \frac{\sum_{i=1}^{r} x_{ii} - \sum_{i=1}^{r} (x_{i+} * x_{+i})}{N^2 - \sum_{i=1}^{r} (x_{i+} * x_{+i})}$$

Where:

r	*Number of rows in the error matrix;*
x_{ii}	*Number of observations in row I and column i;*
x_{i+}	*Total of observations in row i;*
x_{+i}	*Total of observations in column i;*
N	Total number of observations included in matrix.

A map accuracy assessment could not be carried out for the reason that no fieldwork was done out and no other ground truth data was available.

4.3.5 Post Classification Processing

In this step the MLC outcomes were further processed in order to employ change detection. Due to the existence of agricultural subclasses these subclasses were merged to an agricultural land class in both outcomes. Furthermore a post-classification smoothing was applied. One applies such a smooth filtering if a thematic map has a somewhat salt and pepper appearance often caused by the used pixel-by-pixel classification algorithm.

A typical example in this study is the presence of scattered pixels, classified as forest in an almost homogenous area labelled as agricultural land due to the approximately similar spectral signatures of forest and cropland. In order to exclude those scattered pixel a majority filter was applied based on logical operations.

The majority filter employs a moving window that passes through the classification outcome. In this study the moving window was set to a 5x5 size. If the middle pixel does not belong to the majority class the pixel will be assigned to the majority class within the window. When the window moves through the data set the original pixel values are constantly used not the modified. If no majority class exists the middle pixel will not be changed (Lillesand et al., 2000).

Additionally, all unclassified pixels in both MLC outcomes were masked out in order to segregate those pixel from the following change detection arithmetic operation.

4.4 Change Detection

A post classification change detection analysis was performed in a GIS. It is a comparative analysis of independently produced classifications of different dates via a simple mathematical combination pixel by pixel. The outcome was a matrix of change classes. The outcomes of both classifications were assigned to values ranging from 1-5, where 1 is forest, 2 is soil, 3 is water, 4 is agriculture and 5 is urban. In figure 4 is illustrated the employed change detection combination. It contains of the following three steps. The first step is a reclassification of the land cover map of 1987 by multiplying the original values with a factor of 10 in order to be able to carry out a subsequent comparison. In the second step a simple addition of both the reclassified outcome of 1987 with values ranging from 10 – 50 and the outcome of 2001 with values ranging from 1-5 was applied. In the last step all pixel values, which indicate no change such as 11, 22, 33, 44 and 55 were reclassified as 0. Thus one can detect changes from a LULC class to a different class due to the calculated cell values. A cell value 12 means that it was

classified as forest in 1987 and in 2001 as agriculture. In brief the cell changed from forestland in agricultural land over the observed period.

The change detection outcome was transformed to vector data and implemented in a geodatabase for the reason that vector data warranties an improved mapping in a GIS.

For cartographic visualisation a spatial threshold was used. The threshold was applied to exclude too small polygons that will make the outcome map unreadable. It is recommended by different authors and corresponds to proper cartographical editing.

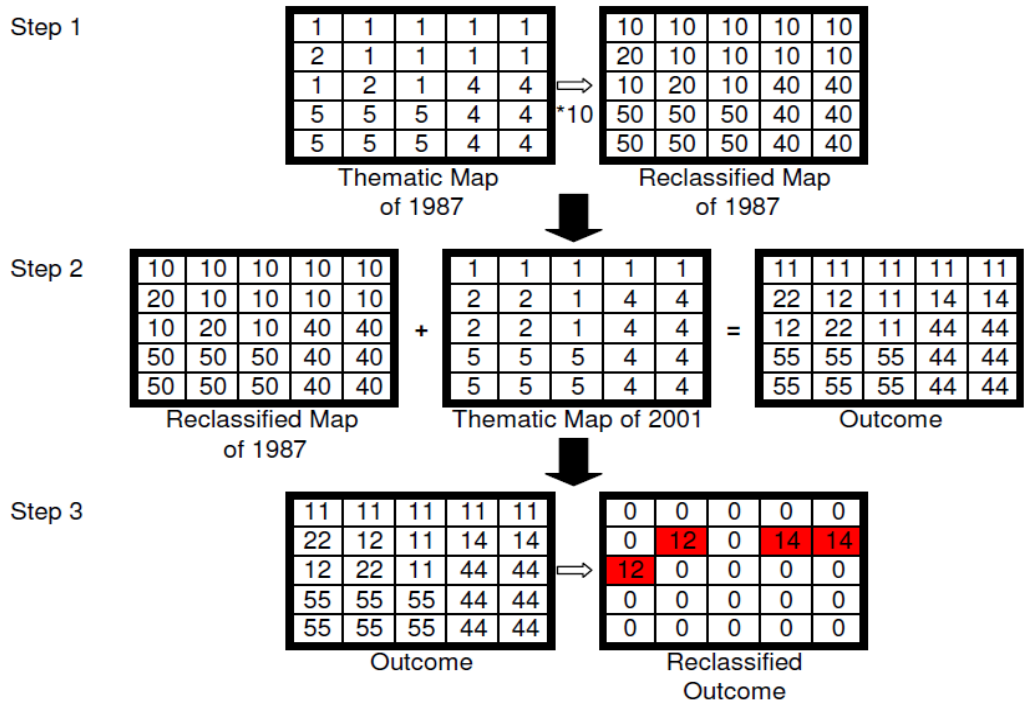

Figure 4 Post-Classification Change Detection Scheme

The applied threshold was two hectares (ha) that means all polygons smaller than an area of two ha were kept out. That led to a total exclusion of change classes related to water due to their marginal spatial appearance and extent respectively.

In the end an adequate map was produced according to proper cartographical conventions in order to achieve a concise visualisation and a clear readability of the change detection map of Imathia. The change classes were coloured in appropiate colours by using an internet based colour brewer hosted by the Pennsylvania State University.

5. Results

5.1 Maximum Likelihood Classification

The outcomes of both classification matrixes allow a comparison of the degree of spatial extent. This area knowledge helps to get an impression of the data distribution. Both MLC outcomes are mapped in the Appendix Maps II and III. Additionally, in figure 5 is displayed the land cover distribution of both classification results in ha (%).

LULC OF Imathia 1987

Apparently agriculture is the dominating LULC in 1987. It occupies 73455 ha (43.9%) of the area and it is located in the lowland of Imathia. The second largest LULC is forest and covers 48652 ha (29.1%). It is mainly situated in Imathias mountainous parts to the west and the southwest. Soil is the third largest LULC and is represented of 32475 ha (19.4%). It has a heterogeneous distribution and is classified mainly in the higher elevated mountainous parts to the west and southwest. In the lowlands it seems to have a scattered distribution with a slightly distribution trend along agricultural land.

The fourth largest LULC is urban and has an area of 12404 ha (7.4%). It is mostly located in the lowland and valleys along the rivers. Additionally, a large urban spot next to the Thermaikos Gulf was classified. The smallest LULC class is water and has an area of 463 ha (0.3%) and is located in the valley in the southwest.

LULC Of Imathia 2001 and differences from 1987

Agriculture is the largest LULC and has a decreased area of 63822 ha (38.1%). It is mostly situated in the lowland but there are a lot of areas scattered in the mountainous parts of Imathia. The second largest LULC is forest with an increased area of 61848 ha (37%). Forest is extended located in the mountainous parts, whereas new areas occurred in the lowland. Soil is the third largest LULC class and increased faintly to an area of 33127 ha (19.8%). It covers less area in the mountainous parts and more spots in the lowland. Urban decreased slightly to 7960 ha (4.8%) and contains changes in its distribution. The large urban spot next to the Thermaikos Gulf disappeared completely as well as infrastructure based structures (e.g. highways or urban fabrics along the rivers). Besides, it gained areas in the mountainous parts. The smallest LULC class is water and increased slightly to 562 ha (0.3%) and has no mentionable spatial distribution changes.

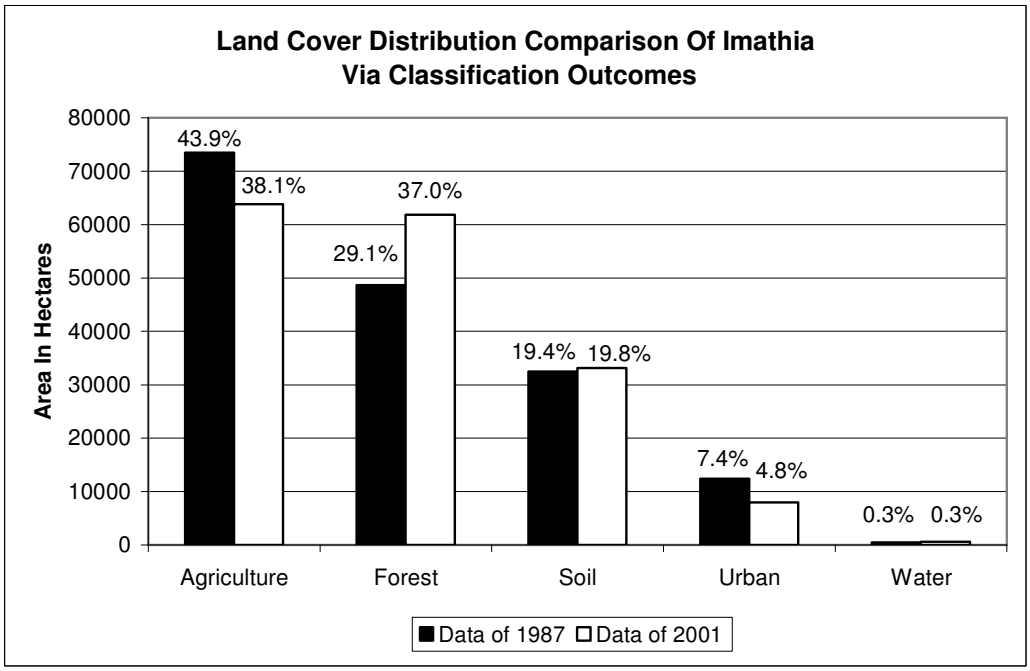

Figure 5 Land Cover Distribution Of Imathia Obtained Via Classification

5.2 Post-classification Change Detection

In order to locate the monitored LULC changes a change detection map is illustrated in the Appendix Maps IV. A detailed area change of each LULC class is listed in table 4. Figure 6 illustrates the areal gain and loss of the generalised LULC change classes over the observed time period. It should be considered slightly differences in the areas between figure 5 and 6 due to the transformation from raster into vector data. A subtraction of gain and loss of each class (see textboxes in figure 6) approximately equals to the observed differences in figure 5.

General Loss

The highest areal loss is detected in agricultural land by 23065 ha (43.5%). Secondly, soil lost area by an extent of 18622 ha (35.1%) followed by urban with 9308 ha (17.5%). Forest has the smallest area of 2083 ha (3.9%) that changed to a different class.

General Gain

Soil achieved the biggest area with an amount of 19188 ha (36.1%). The second highest gain is located in the forest class with an extent 15089 ha (28.4%) followed by the agriculture class 13831 ha (26.1%). The urban class obtained the smallest area with 4970 ha (9.4%).

A comparison of gains and losses shows three main LULC changes. The first is a clear area gain of forest by approximately 13000 ha. The second change is an area loss of agriculture by an extent of approximately 9200 ha and of urban by an extent of approximately 4300 ha. The third change represents a little change of the soil class for the reason that it achieved a very small area of approximately 500 ha.

Detailed LULC Changes

Since some classes (e.g. soil) have a high gain and loss at the same instance it is feasible to provide a detailed representation of LULC class changes. A detailed illustration points how LULC has changed (i.e. from which class to which class). This is useful to control the informational value of a LULC change in order prove if a detected change make sense and its spatial extent. In table 1 is shown to what spatial extend each LULC classes changed.

Major spatial extents have 'agriculture to soil' of 14646 ha (27.6%), 'soil to forest' of 9769 ha (18.4%) and 'soil to agriculture' of (14.4%). Rather small changes have 'urban to agriculture' of 5172 ha (9.7%), 'agriculture to forest' 4827 ha of (9.1%), 'urban to soil' 3644 ha of (6.9%) and 'agriculture to urban' of 3591 ha (6.8%).

Whereas very small changes are located in 'soil to urban' of 1223 ha (2.3%), 'forest to agriculture' of 1029 ha (1.9%), 'forest to soil' of 898 ha (1.7%), 'urban to forest' of 493 ha (0.9%) and in the 'forest to urban' class of 156 ha (0.3%).

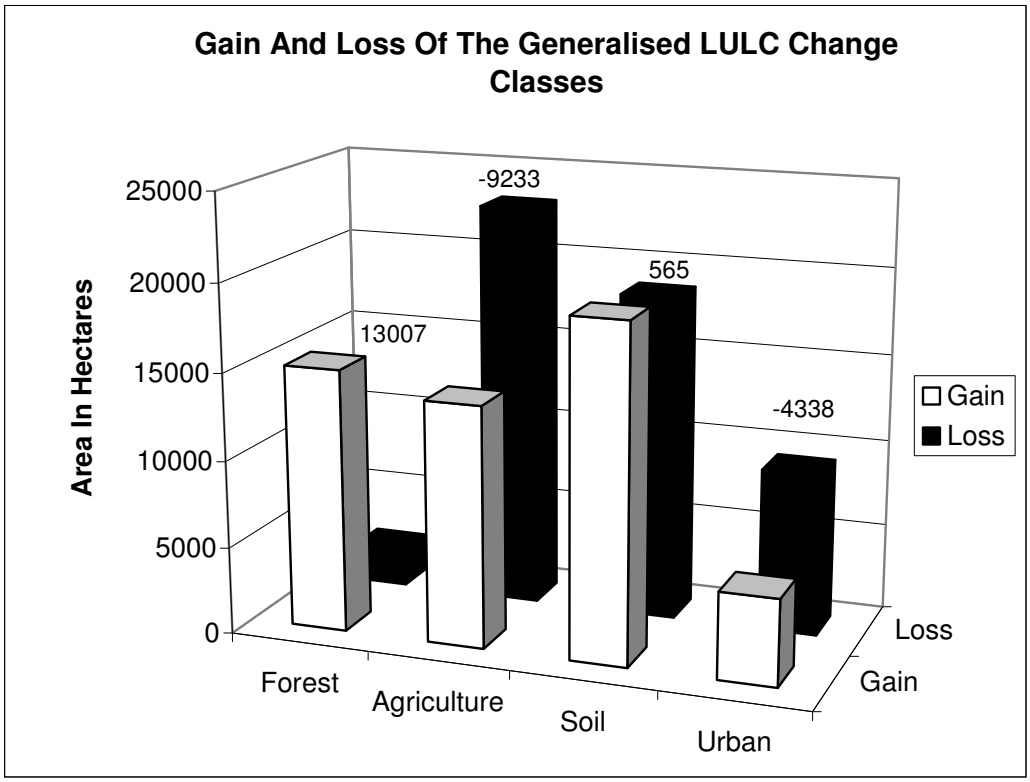

Figure 6 Areal Gain And Loss Of Generalised LULC Change Classes

Table 4 Detailed Change of Detected LULC Classes

LULC Change Classes	Area in hectares	Area in percentage
Forest to Urban	156	0.3
Urban to Forest	493	0.9
Forest to Soil	898	1.7
Forest to Agriculture	1029	1.9
Soil to Urban	1223	2.3
Agriculture to Urban	3591	6.8
Urban to Soil	3644	6.9
Agriculture to Forest	4827	9.1
Urban to Agriculture	5172	9.7
Soil to Agriculture	7630	14.4
Soil to Forest	9769	18.4
Agriculture to Soil	14646	27.6

6. Discussion

This post-classification change detection offers a multitude of LULC changes in this study area. Two of the main LULC changes are chosen in order to discuss how and to what spatial extent they have changed. Furthermore will be discussed the representativeness and error sources that influence the result of this study.

First Main Change (To Forest)

The Results of the LULC class change show a high area achievement and a very small loss of the 'to forest' class. The change detection map helps to locate those spots of change and to use the detailed source classes. The spots consist of the source soil and agriculture class and are mostly located in the mountainous parts of the study area. This can be explained by forestation of former agricultural land or soil class spots (e.g. ruderal vegetation, shrub-land etc.), which were probably affected by wildfires and vegetated over time. The highest amount of achievement is based on 'soil to forest' (18.4%) what seems to be a possible LULC change in a logical point of view due to its location in the mountainous parts in southwest of Imathia.

In contrast, the change of 'agriculture to forest' (9.1%) located in the lowland is difficult to interpret since the main irrigated crops in Imathia are peach, pear and apple trees (Albanis et al. 1996). This means a similar spectral signature of forest trees and those agricultural trees can be expected by using Landsat ground resolution. On the other hand, the detected changes can be caused of changes in financing support from European Union according to Vasilakos (personal communication, 08/01/2009).

'Urban to forest' (0.9%) is a very small change and can be neglected. Moreover it occurs seldom in reality.

On the other hand the seasonal difference of the satellite data should be taken into account as an error source. Related to that is the ground resolution of Landsat data. It implies a mixture of several spectral signatures in a pixel (compare Lillesand et al., 2000 and Richards and Jia, 1999).

Second Main Change (To Agriculture)

The 'to agriculture' change class is chosen to represent the second main change since it achieved more area than the 'to urban' class. The highest gain is mainly caused of 'soil to agriculture' (14.4%) and is basically located in the mountainous parts to the southwest (compare change detection map). This change should be handled with care since the sub-classes of agriculture (i.e. crop-land and arable-land) have a mentionable probability of spectral signature overlapping with the soil class (e.g. ruderal vegetation and sparsely vegetated spots) in the multi-spectral feature space. That overlapping could not be excluded during the spectral signature developing process since some overlaps are natural according to Lillesand et al. (2000). Higher elevated areas, where the change took place, are uncommon for agricultural land use since it is difficult to provide and maintain infrastructure such as irrigation networks. Furthermore the mixture of several spectral signatures should be considered. Seasonal differences were tried to exclude due to the application of agricultural sub-classes but spectral signatures overlap between ruderal vegetation and young crops are likely and lead to misclassification.

The second highest gain was achieved from 'urban to agriculture' (9.7%) and does not make sense in a logical point of view. It is very unlikely that urban areas are removed for agricultural land use. This unreal change phenomenon is caused by a misclassification of the TM imagery due similar spectral signatures of urban surfaces and agriculture (i.e. arable-land) in the dry summer. It is mainly located in the coastal area of Imathia and along the Aliakmon river.

'Forest to agriculture' (1.7%) has a negligible small gain and its distribution is mainly located in the lower elevated areas of the mountainous parts in Imathia. It could be a result of deforestation in order to achieve arable land or a process of forest management. On the other hand it can be caused of spectral signature similarities between agriculture (i.e. cropland) and a newly planted forest.

In other words no considerable change of agriculture can be assumed and this corresponds to Vasilakos (personal communication, 08/01/2009). Vasilakos mentioned that no major problems (e.g. land abandonment) exist in Imathia, which could lead to rapid LULC changes in Imathia.

Representativeness

The main result of this study is an increase of forest since the main forest class has the highest increase of area. Basically, detailed LULC change classes that lead to forest make sense (e.g. 'soil to forest' and 'agriculture to forest').

On the other hand, that conclusion is based on two points in time and rises the question of the representativeness. In figure 8 is illustrated (Appendix Figures) a fictional LULC change development over a period of 50 years in order to demonstrate this question. It contains increases and decreases of LULC change rates. Two points (1987 and 2001) are selected for a LULC study and the result will apparently show a decrease in LULC change rates (dashed line). Considering the whole time series there is no decrease in LULC change rate and the chosen two points in time are non-representative. That means more satellite data are needed for a representative LULC change detection analysis of Imathia. In an exemplary study Helldén and Tottrup (2008) observed steadily the loss of vegetation cover and the biomass productivity over a time period from 1981 to 2003 and consider the results as non-representative.

Map Accuracy Assessment

An Achilles' heel of this study is the missing map accuracy assessment. Unreal change phenomena possibly will occur in the change detection due to a low classification quality. Examining a map accuracy assessment is strongly recommended (Lillesand et al, 2000 and Richards and Jia, 1999).

Since no ground truth data are available one can refer to a case study of agricultural fields in Greece (Lesvos island). It was employed a MLC on TM data and the classification accuracy assessment performed well (Vasilakos et al., 2004). Differences of physical settings between the study areas cannot be neglected.

Furthermore have been carried out studies by using TM and ETM+ data and applying MLC with adequate map accuracy assessments (Hall et al., 1991; Hall and Knapp, 1999 and Her, Y. 2007).

The classification accuracy of the LULC map of Imathia in 1987 is probably rather poor than well for the reason that areas were misclassified and an iterative spectral signature enhancement improved the MLC results marginal. As an example obviously agricultural land was classified as urban and led to unreal change phenomena (e.g. 'urban to agriculture'). It is assumed such a poor accuracy for the MLC of 2001, as well.

Seasonal Difference

Since the first image was recorded in July 1987 (19/07/1987) one can expect dry and hot climate conditions. The second image was gathered in May 2001 (30/05/2001) that implies for example more 'greenness' in the spectral signature due to higher water availability (i.e. precipitation) and lower temperatures compared to the summer season (see figure 1). A comparison of summer and spring images leads to a different appearance of the same LULC class or vegetation type. The approach of selecting seasonal independent spectral classes could reduce but not avoid errors. The acquisition dates of the imagery are apparently not anniversary dates and thus inadequate for the employed change detection analysis. In fact, this led to the mentioned errors in the change detection analysis. The image acquisition is one of the most important points of change detection analysis and even satellite data of anniversary dates do not ensure a representative comparison (Coppin et al. 2004).

However, imagery acquisition was restricted due to limited Landsat data availability of the study area at GLCF.

Ground Resolution and Spectral Mixture

The classification quality is strongly limited on the spatial resolution of TM and ETM+ data and the quality of change detection results, consequently. This highlights the question if TM and ETM+ ground resolution enables an appropriate LULC mapping with MLC on this scale. Spectral mixtures of various features fall within a TM 30m pixel and act as error sources (Hall and Knapp, 1999) in heterogeneous and sparsely vegetated landscapes like the Mediterranean basin. Confusing background soil signatures occurred mostly in the mountainous parts of Imathia that are not covered with forest and tend to be sparsely vegetated.

Resulting misclassifications can be placed in overlapping spectral signatures of the spectral classes since spectrally pure classes are seldom recorded in multi-spectral satellite data (Emmanouloudis et al., 2007). Therefore one should consider other approaches that can be used for LULC monitoring.

Studies have been carried out and performed well involving a spectral mixture analysis (SMA) in order to solve the spectral mixing of various features, such as separating grassland and shrub vegetation in TM and ETM+ data (Hostert et al., 2003; Kuemmerle et al., 2006[a] and Röder et al., 2007). Detailed explanations of SMA are given in Lillesand et al. (2000) and Richards and Jia (1999).

Moreover it is possible to employ the technique of hybrid classification. Hybrid classification combines the advantages of supervised and unsupervised classification algorithms. In Lillesand et al. (2000) and Richards and Jia (1999) are specified detailed descriptions of hybrid classification. Kuemmerle et al. (2006[b]) applied an advanced hybrid classification technique in Eastern Europe using TM and ETM+ data and the approach performed well.

Image Interpreter

Carrying out a monitoring study is influenced by individual interpretations. Personal decisions manipulate data selection, workflow and interpretation of the results as well as comparison with different studies.

MLC applied on remotely sensed data needs a lot of input variables, which are strongly influenced by the subjective opinion and determination of the image interpreter. In the following will be described the most important personal decisions that have influenced the results of this study.

The selection of the used sensor system as well as the data acquisition is based on an individual decision. Information classes were defined subjectively. Image enhancement steps like PCA, WDVI (i.e. definition of the soil line) and FCC's need input data that are selected individually. The determination of training sites in order to produce spectral signatures and their improvement were strongly influenced by the image interpreter. The determination of training sites is art and science (Lillesand et al., 2000). Post-classification procedures and decision of a threshold for excluding the vector data were defined subjectively. The same study performed by a different student might have disagreeing results.

Potential Of Approach

This study shows a weak potential of MLC, applied on TM and ETM+ data, in this heterogeneous study area to indicate LULC changes. On can assume one real change phenomenon of increased forest under the given conditions. However, missing map accuracy assessments and the question of representativeness lead to handle this assumption with care. So far no mentionable LULC studies, based on remotely sensed data, have been conducted in Imathia. Therefore a meaningful comparison of this study results and other results is hardly accomplishable.

The other discussed changes are assumed as unreal phenomena since they offer weak informational values. They could not be validated with map accuracy assessments and compared to other studies.
The potential of this approach could be improved with adequate fieldwork data in order to define better information and spectral classes. Furthermore would be a focus either on the lowland or the mountainous parts helps to solve spectral signature overlapping problem due to the heterogeneity of this study area.

On the other hand, it is suggested to employ more advanced classification techniques to monitor LULC changes (Ediriwickrema and Khorram, 1997; Symeonakis et al., 2004; Kuemmerle et al. 2006[b]; Emmanouloudis et al., 2007) and a higher temporal resolution (Hostert et al., 2003). In addition, higher-ground-resolution satellite imagery could be used to detect LULC changes in this small-structured study area. However, high-resolution data would still have its imperfections.

7. Conclusion

The post-classification change detection analysis monitored an increase of forest in this study area under the given data conditions. Other observed changes are assumed as unreal phenomena caused of uncertain source classes, spectral signature overlapping in the multi-spectral feature space during the classification and seasonal differences.

The MLC of TM and ETM+ produced two qualitative measurements of the defined LULC classes. The performance of MLC could not be validated via a map accuracy assessment and a multitude of unreal change phenomena lead to the assumption of a poor classification quality.

The chosen mathematical combination of the two classifications carried out well in order to detect gain and loss of LULC classes and to locate changes on a map. The vectorised LULC change areas can be used for further detailed investigations, such as land degradation studies. Provided that the classifications would perform well.

The post-classification change detection analysis performed weakly to indicate changes of LULC in such a small-structured and heterogeneous study area.

8. Literature

Books

Brandt, C.J. and Thornes, J.B (eds) 1996, Mediterranean Dersertification and Land Use. John Wiley & Sons, Chichester.

Jensen J.R. 1996, Introductory Digital Image Processing: A Remote Sensing Perspective. 2ndEdition, Prentice-Hall, Upper Saddle River, NJ.

Kramer, H.J. 2001, Observation of the Earth and its Environment. Survey of Missions and Sensors. Springer, Berlin/Heidelberg/ New York.

Lillesand, T.M. and Kiefer, R.W., Chipman J.W., 2000, Remote Sensing and Image Interpretation. John Wiley & Sons, New York.

Richards, J.A.. and Jia, X., 1999, Remote Sensing Digital Image Analysis: An Introduction. 3rd Edition, Springer, Berlin/Heidelberg/New York.

Articles

Albanis, T.A., Hela, D.G., Sakellarides, T.M and Konstantinou, I.K., 1998, Monitoring of pesticide residues and their metabolites in surface and underground waters of Imathia (N. Greece) by means of solidphase extraction disks and gas chromatography. Journal of. Chromatography A, vol. 823, pp. 59-71 (13).

Baldridge, A.M., Hook, S J., Grove, C.I. and Rivera, G., 2009, The ASTER Spectral Library Version 2.0. In press Remote Sensing of Environment.

Chander, G., and Markham, B., 2003, Revised Landsat-5 TM Radiometric Calibration Procedures and Postcalibration Dynamic Ranges. IEEE Transactions on Geoscience and Remote Sensing, vol. 41, no. 11, pp. 2674-2677.

Coppin, P., Jonckheere, I., Nackaerts, K., Muys, B. and Lambin. E., 2004, Digital change detection methods in ecosystem monitoring: A review. International Journal of Remote Sensing, vol. 25, no. 9, pp. 1565-1596 (32).

DongMei, C. and FitzGibbon, J., 2008, Comparison of seasonal change detection from multi-temporal MODIS and TM images in Southern Ontario. Earth Observation and Remote Sensing Applications, 2008. EORSA 2008. International Workshop on , vol., no., pp.1-6, June 30 2008-July 2 2008.

Emmanouloudis, D.A., Myronidis D.I., Panilas, S.Ch. and Takos, I.A., 2007, Identification of the climate change effect on Nestos Delta (N.Greece) by using remote sensing, water analysis and GIS Techniques. Journal of International Research Publications, Vol 2, Issue Ecology, pp 21-31.

Ediriwickrema, J. and Khorram, S., 1997, Hierarchical maximum-likelihood classification for improved accuracies. IEEE Transactions on Geoscience and Remote Sensing, vol. 35, no. 4, pp. 810-816.

Fung, T. and LeDrew, E., 1987, Application of principal components analysis change detection. Photogrammetric Engineering and Remote Sensing, vol.53, pp. 1649- 1658.

Hall, F.G., Botkin, D.B., Strebel, D.E., Woods, K.D. and Goetz, S.J., 1991, Large-scale patterns of forest succession as determined by remote sensing. Ecology, vol. 72, no. 2, pp. 628-640.

Hall, F. G. and Knapp D., 1999, BOREAS TE-18 Landsat TM Maximum Likelihood Classification Image of the SSA. Data set. Available online [http://www.daac.ornl.gov] from Oak Ridge National Laboratory Distributed Active Archive Center, Oak Ridge, Tennessee, U.S.A.

Helldén, U. and Tottrup, C., 2008, Regional desertification: A global synthesis. Global and Planetary Change, vol.64, pp. 169-176.

Her, Y., 2007, Land use classification in Zambia using Quickbird and Landsat imagery. ASABE Paper No. 072017.

Hostert, P., Roder, A. and Hill, J., 2003, Coupling spectral unmixing and trend analysis for monitoring of long-term vegetation dynamics in Mediterranean rangelands. Remote Sensing of Environment, vol. 87, pp. 183−197.

Karyotis, Th., Panagopoulos, A., Alexiou, J., Kalfountzos, D., Pateras, D., Argyropoulos, G. and Panoras, A., 2006, Nitrates pollution in a vulnerable zone of Greece. Communications in Biometry and Crop Science, vol. 1, no. 2, pp. 72-78.

Kuemmerle, T., Röder, A. and Hill, J., 2006[a], Separating grassland and shrub vegetation by multidate pixel-adaptive spectral mixture analysis. International Journal of Remote Sensing, vol. 27, pp. 3251−3271.

Kuemmerle, T., Radeloff, V.C., Perzanowski, K. and Hostert, P., 2006[b], Cross-border comparison of land cover and landscape pattern in Eastern Europe using a hybrid classification technique. Remote Sensing of Environment, vol. 103, pp. 449–464.

Lorent, H., Evangelou, C., Stellmes, M., Hill, J., Papanastasis, V., Tsiourlis, G., Roeder, A., and Lambin, E.F., 2008, Land degradation and agricultural households in a marginal region of northern Greece. Global and Planetary Change, vol 1383, in press.

Röder, A., Kuemmerle, T., Hill, J., Papanastasis, V.P. and Tsiourlis, G.M., 2007, Adaptation of a grazing gradient concept to heterogeneous Mediterranean rangelands using cost surface modelling. Ecological Modelling, vol. 204, pp. 387−398.

Röder, A., Udelhoven, Th., Hill, J., del Barrio, G. and Tsiourlis, G., 2008, Trend analysis of Landsat-TM and -ETM+ imagery to monitor grazing impact in a rangeland ecosystem in Northern Greece. Remote Sensing of Environment, vol. 112, no. 6, pp. 2863-2875.

Salvati, L. and Zitti, M., 2008, Assessing the impact of ecological and economic factors on land degradation vulnerability through multiway analysis. Ecological Indicators, vol. 9, pp. 357 –363.

Song, C., Woodcock, C.E., Seto, K.C., Lenney, M.P. and Macomber, S.A., 2001, Classification and Change Detection Using Landsat TM Data: When and How to Correct Atmospheric Effects? Remote Sensing of Environment, vol. 75, no. 2, pp. 230-244.

Symeonakis, E., Koukoulas, S., Calvo, C.A., Arnau, R.E. and Makris, I., 2004, A landuse change and land degradation study in Spain and Greece using remote sensing and GIS. International Archives of Photogrammetry, Remote Sensing and Spatial Information Sciences, vol. 35 (Part B7), pp. 553–558.

UNCED 1992: Report of the United Nations Conference on Environment and Development, Chapter 12: Managing fragile ecosystems: Combating desertification and drought- (Rio de Janeiro, 3–14 June 1992), General A/CONF.151/26 (Vol. II), Chapter 12.

Vasilakos, C., J. Hatzopoulos, K. Kalabokidis, K. Koutsovilis, and Thomaidou. A., 2004, Classification of agricultural fields by using Landsat TM and QuickBird sensors. The case study of olive trees in Lesvos Island. In Proceedings International Conference on Information Systems, & Innovative Technologies in Agriculture, Food and Environment, Vlachopoulou et al. (ed.), 18-20 March 2004, Hellenic Association of Information and Communication Technology in Agriculture, Food and Environment (HAICTA), Thessaloniki, Greece. vol. 2, pp. 324-332.

Internet Data Sources

Colorbrewer hosted by the Pennsylvania State University last

Accessed: 12/05/2008

Available:: http://www.colorbrewer.org

Global Land Cover Facility - Landsat 5 Thematic Mapper Data,

NASA Landsat Program, 2001, Landsat TM scene p184r32_5t19870719, L1G - GeoCover - Orthorectified, USGS, Sioux Falls, 07/19/1987.

Accessed: 01/11/2008

Available: http://glcfapp.umiacs.umd.edu:8080/esdi/index.jsp

Global Land Cover Facility - Landsat 7 Enhanced Thematic Mapper Plus Data

NASA Landsat Program, 2004, Landsat ETM+ scene p184r032_7k20010530, L1G - GeoCover - Orthorectified, USGS, Sioux Falls, 05/30/2001.

Accessed: : 01/11/2008

Available: http://glcfapp.umiacs.umd.edu:8080/esdi/index.jsp

Hellenic National Meteorological Service – Climatic Data of Trikalas (Imathia) Accessed: 20/12/2008

Available: http://www.hnms.gr/hnms/english/climatology/climatology_region_diagrams_html?dr_city=Trikala_Imathia

Additional Sources

Eastman, J. R. 2006, Clark labs, IDRISI Andes Manual and Tutorial, IDRISI The Andes version 15th Edition.

Esri Inc 2008, ESRI® Data & Maps

Pilesjö, P., 1992, GIS and remote sensing for soil erosion studies in semi-arid environments. Estimation of soil erosion parameters at different scales, PhD thesis. Lund University Press, Lund, Sweden, 203.

Vasilakos, C., J, 2009, Personal Communication. Department of Geography ,University of the Aegean (08/01/2009).

Appendix Figures

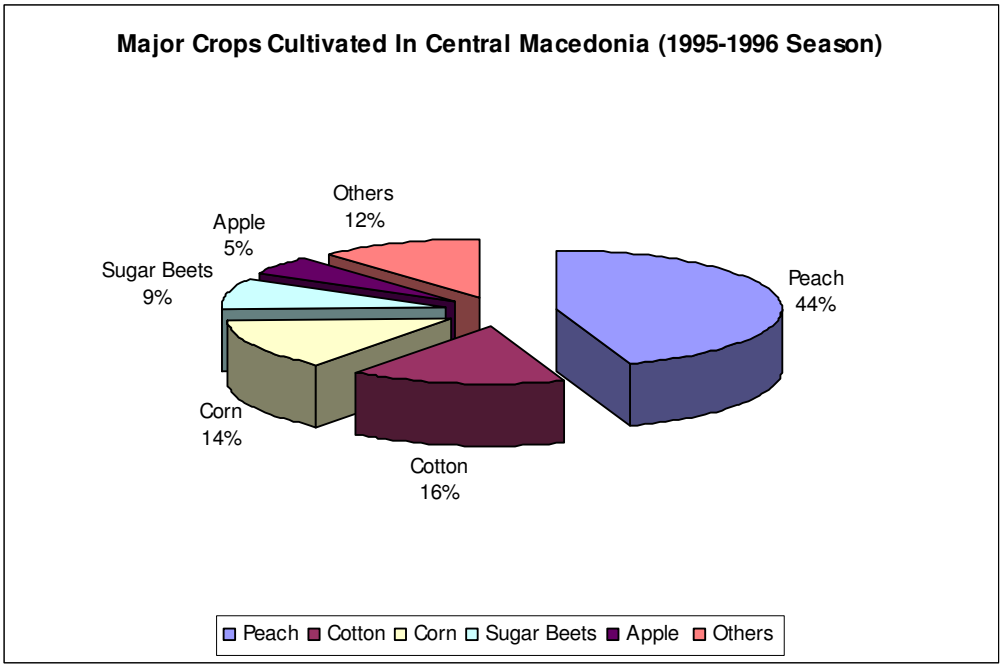

Figure 7 Distribution Of Main Crops in Central Macedonia (Albanis et al. 1998)

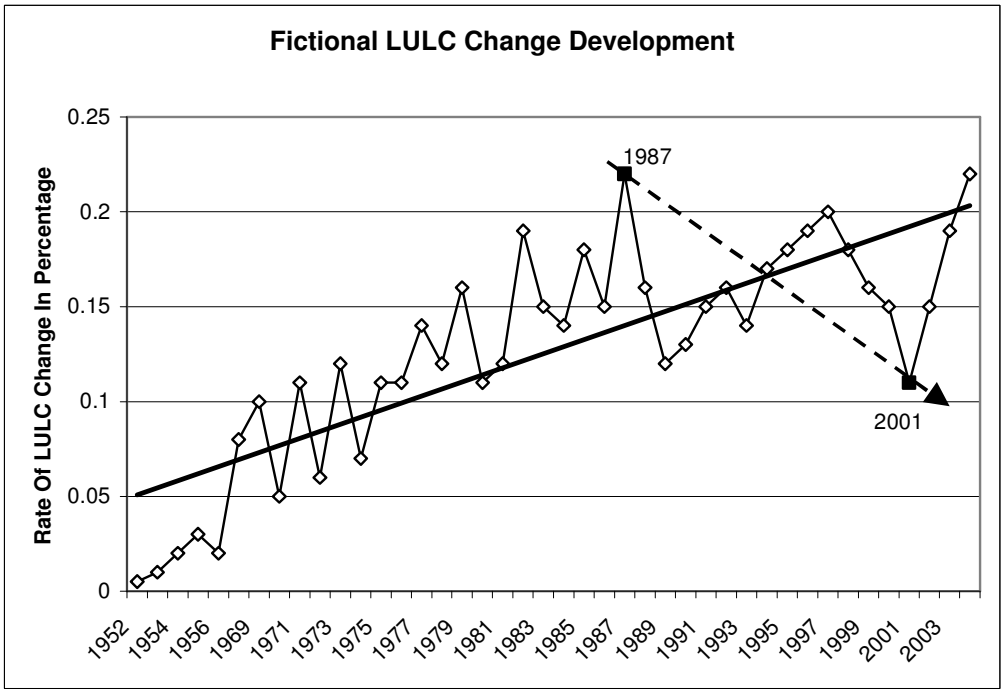

Figure 8 Fictional LULC Change Development

Appendix Maps I Overview Map Of Imathia, Nothern Greece In 2001

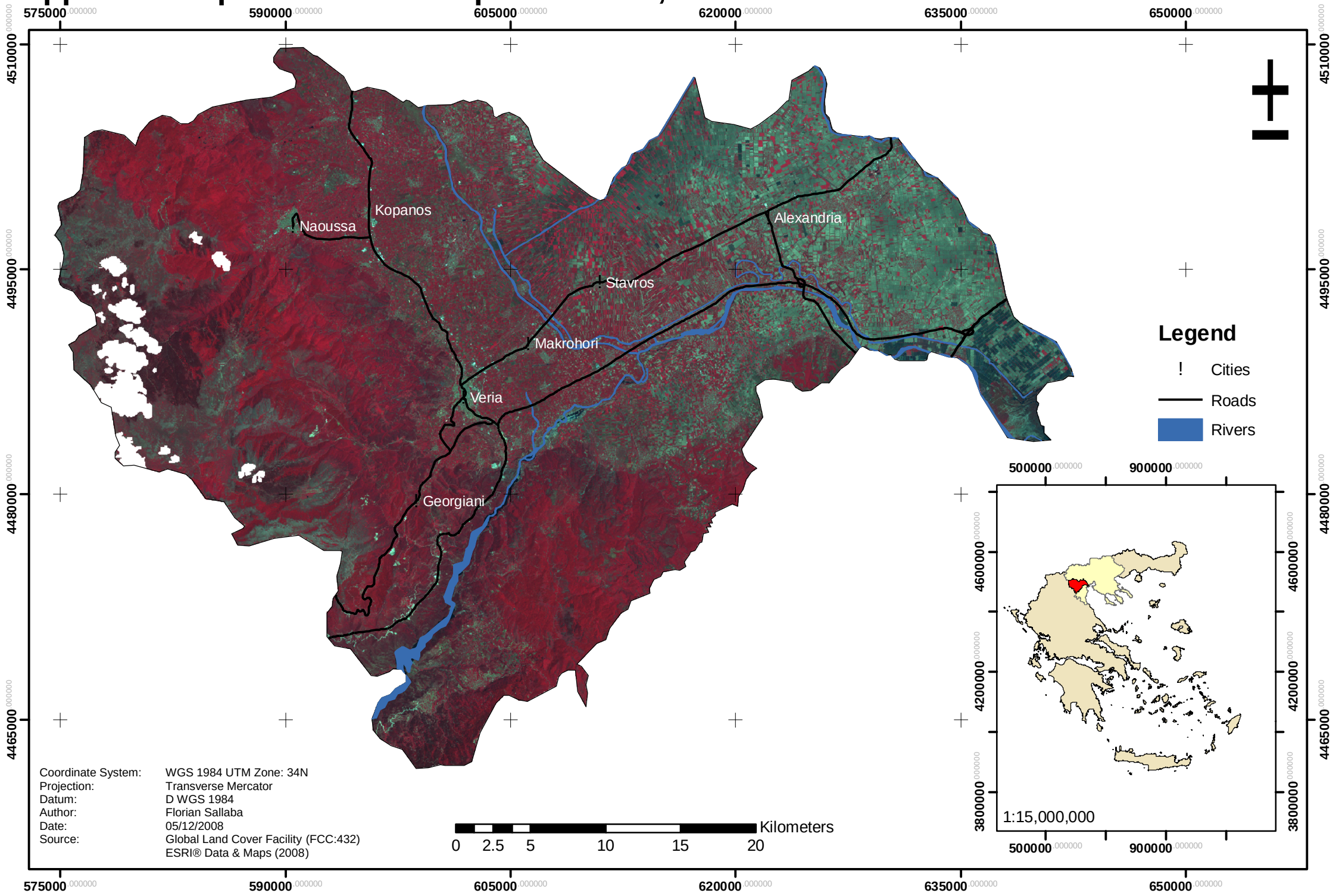

Appendix Maps II LULC Map Of Imathia In 1987

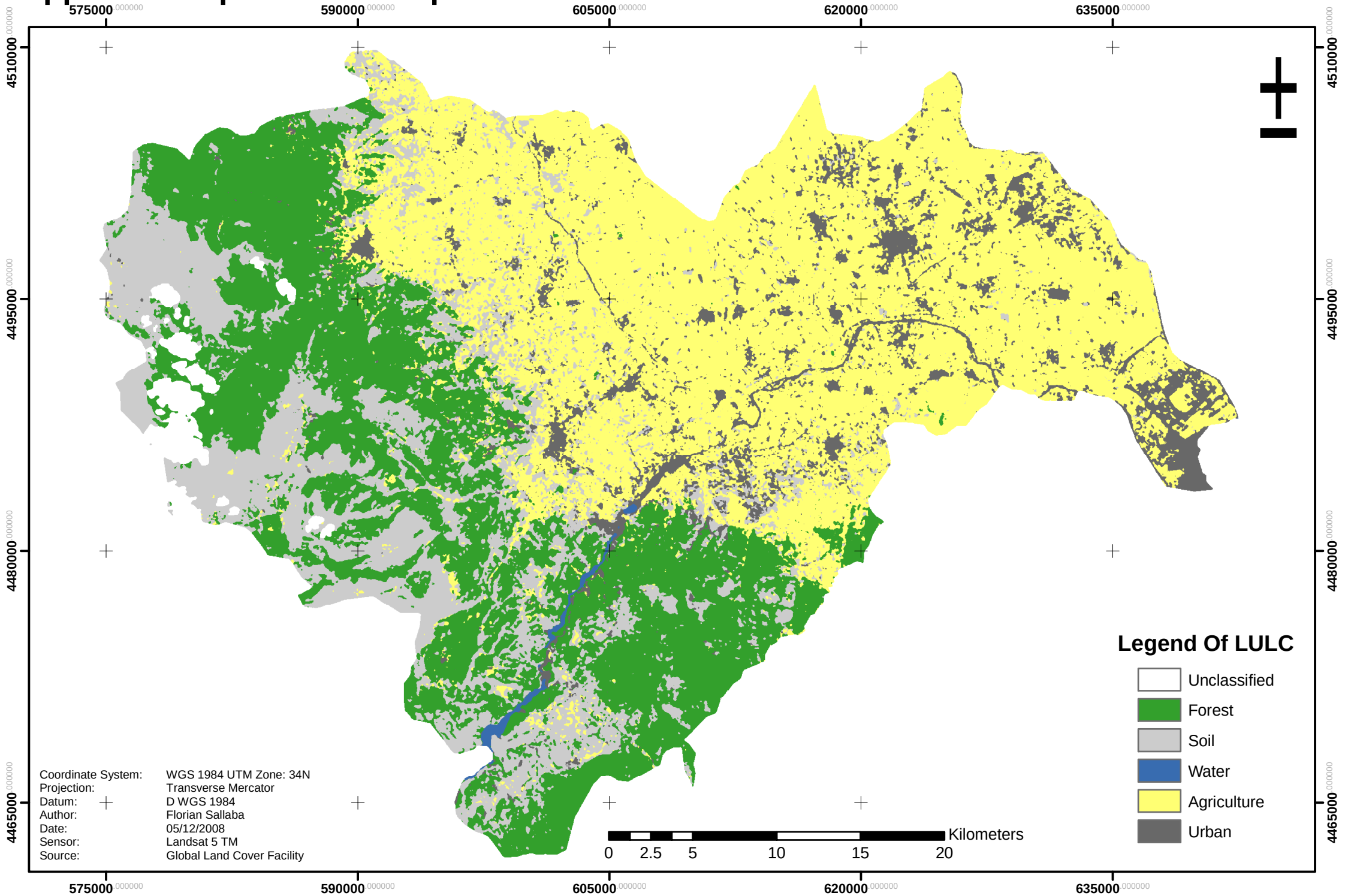

Appendix Maps III LULC Map Of Imathia In 2001

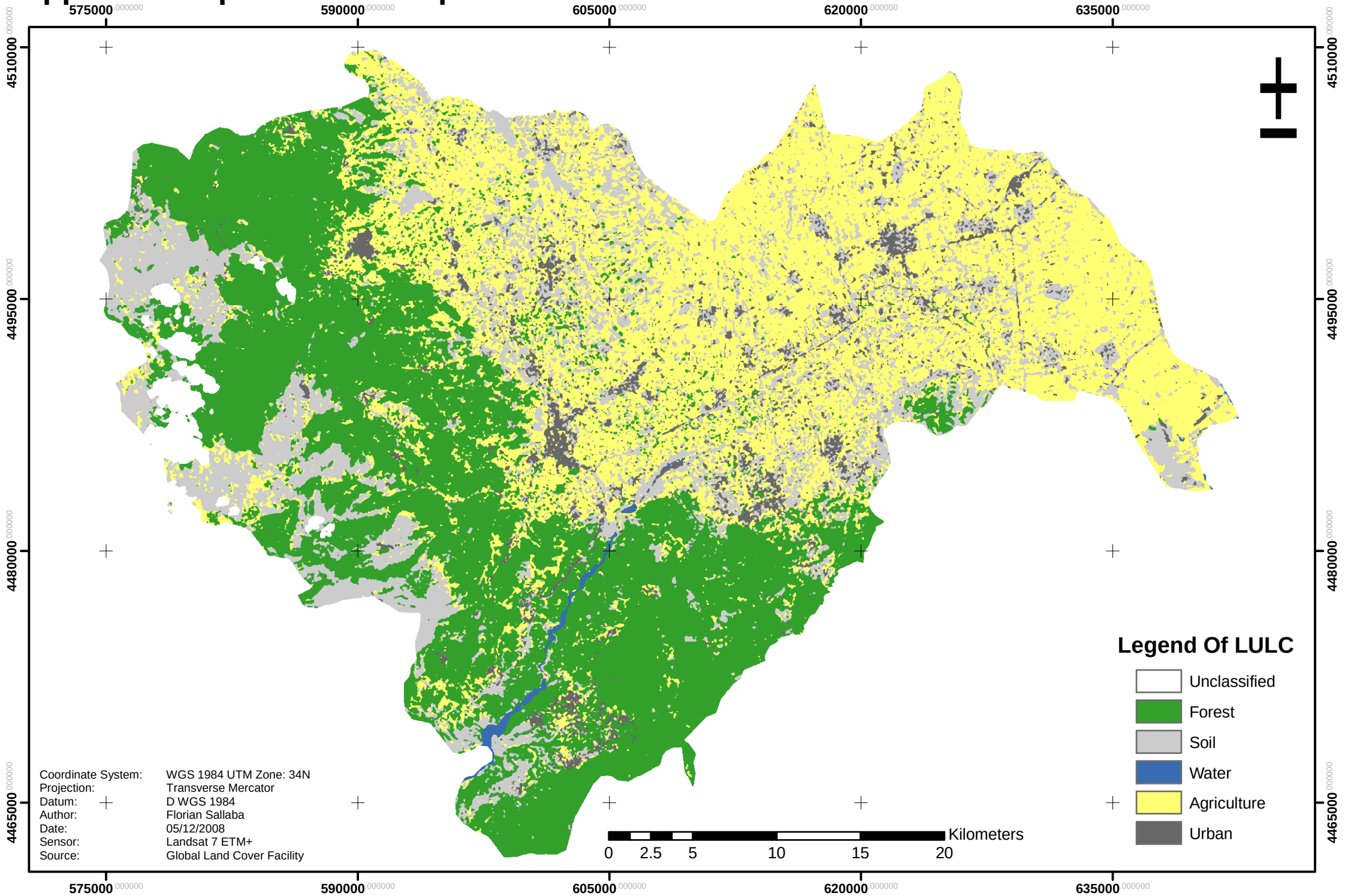

Appendix Maps IV LULC Change Detection Map Of Imathia

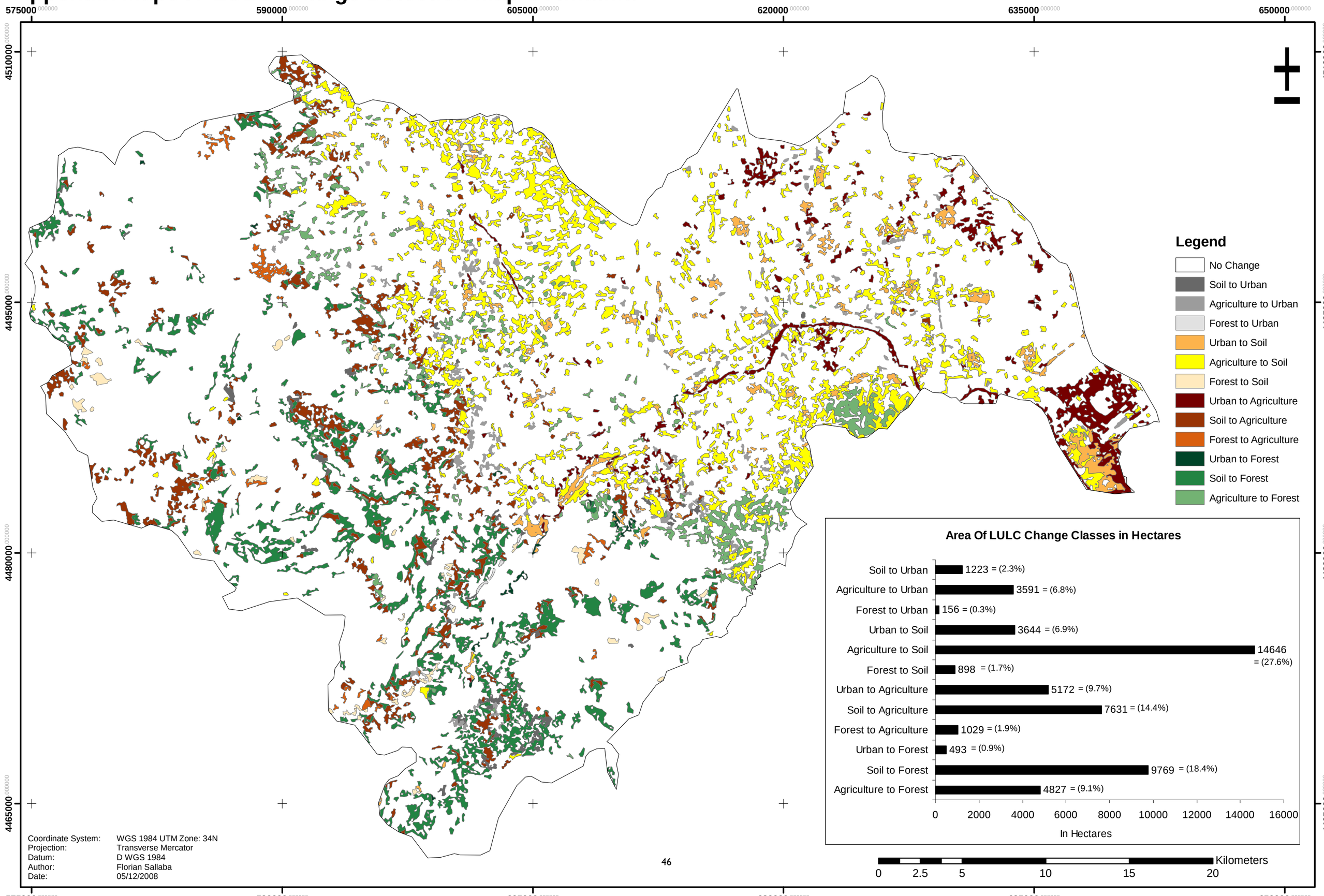

Lunds Universitets Naturgeografiska institution. Seminarieuppsatser. Uppsatserna finns tillgängliga på Naturgeografiska institutionens bibliotek, Sölvegatan 12, 223 62 LUND.
Serien startade 1985. Uppsatserna är även tillgängliga på http://www.geobib.lu.se/

The reports are available at the Geo-Library, Department of Physical Geography, University of Lund, Sölvegatan 12, S-223 62 Lund, Sweden.
Report series started 1985. Also available at http://www.geobib.lu.se/

90. Poussart, J-N., (2002): Verification of Soil Carbon Sequestration - Uncertainties of Assessment Methods.
91. Jakubaschk, C., (2002): Acacia senegal, Soil Organic Carbon and Nitrogen Contents: A Study in North Kordofan, Sudan.
92. Lindqvist, S., (2002): Skattning av kväve i gran med hjälp av fjärranalys.
93. Göthe, A., (2002): Översvämningskartering av Vombs ängar.
94. Lööv, A., (2002): Igenväxning av Köphultasjö – bakomliggande orsaker och processer.
95. Axelsson, H., (2003): Sårbarhetskartering av bekämpningsmedels läckage till grundvattnet – Tillämpat på vattenskyddsområdet Ignaberga-Hässleholm.
96. Hedberg, M., Jönsson, L., (2003): Geografiska Informationssystem på Internet – En webbaserad GIS-applikation med kalknings- och försurningsinformation för Kronobergs län.
97. Svensson, J., (2003): Wind Throw Damages on Forests – Frequency and Associated Pressure Patterns 1961-1990 and in a Future Climate Scenario.
98. Stroh, E., (2003): Analys av fiskrättsförhållandena i Stockholms skärgård i relation till känsliga områden samt fysisk störning.
99. Bäckstrand, K., (2004): The dynamics of non-methane hydrocarbons and other trace gas fluxes on a subarctic mire in northern Sweden.
100. Hahn, K., (2004): Termohalin cirkulation i Nordatlanten.
101. Lina Möllerström (2004): Modelling soil temperature & soil water availability in semi-arid Sudan: validation and testing.
102. Setterby, Y., (2004): Igenväxande hagmarkers förekomst och tillstånd i Västra Götaland.
103. Edlundh, L., (2004): Utveckling av en metodik för att med hjälp av lagerföljdsdata och geografiska informationssystem (GIS) modellera och rekonstruera våtmarker i Skåne.
104. Schubert, P., (2004): Cultivation potential in Hambantota district, Sri Lanka
105. Brage, T., (2004): Kvalitetskontroll av servicedatabasen Sisyla
106. Sjöström., M., (2004): Investigating Vegetation Changes in the African Sahel 1982-2002: A Comparative Analysis Using Landsat, MODIS and AVHRR Remote Sensing Data
107. Danilovic, A., Stenqvist, M., (2004): Naturlig föryngring av skog
108. Materia, S., (2004): Forests acting as a carbon source: analysis of two possible causes for Norunda forest site
109. Hinderson, T., (2004): Analysing environmental change in semi-arid areas in Kordofan, Sudan
110. Andersson, J., (2004): Skånska småvatten nu och då - jämförelse mellan 1940, 1980 och 2000-talet
111. Tränk, L., (2005): Kadmium i skånska vattendrag – en metodstudie i föroreningsmodellering.

112. Nilsson, E., Svensson, A.-K., (2005): Agro-Ecological Assessment of Phonxay District, Luang Phrabang Province, Lao PDR. A Minor Field Study.
113. Svensson, S., (2005): Snowcover dynamics and plant phenology extraction using digital camera images and its relation to CO2 fluxes at Stordalen mire, Northern Sweden.
114. Barth, P. von., (2005): Småvatten då och nu. En förändringsstudie av småvatten och deras kväveretentionsförmåga.
115. Areskoug, M., (2005): Planering av dagsutflykter på Island med nätverkanalys
116. Lund, M., (2005): Winter dynamics of the greenhouse gas exchange in a natural bog.
117. Persson, E., (2005): Effect of leaf optical properties on remote sensing of leaf area index in deciduous forest.
118. Mjöfors, K., (2005): How does elevated atmospheric CO2 concentration affect vegetation productivity?
119. Tollebäck, E.,(2005): Modellering av kväveavskiljningen under fyra år i en anlagd våtmark på Lilla Böslid, Halland
120. Isacsson, C., (2005): Empiriska samband mellan fältdata och satellitdata – för olika bokskogområden i södra Sverige.
121. Bergström, D., Malmros, C., (2005): Finding potential sites for small-scale Hydro Power in Uganda: a step to assist the rural electrification by the use of GIS
122. Magnusson, A., (2005): Kartering av skogsskador hos bok och ek i södra Sverige med hjälp av satellitdata.
123. Levallius, J., (2005): Green roofs on municipal buildings in Lund – Modeling potential environmenta benefits.
124. Florén, K., Olsson, M., (2006): Glacifluviala avlagrings- och erosionsformer I sydöstra Skåne – en sedimentologisk och geomorfologisk undersökning.
125. Liljewalch-Fogelmark, K., (2006): Tågbuller i Skåne – befolkningens exponering.
126. Irminger Street, T., (2006): The effects of landscape configuration on species richness and diversity in semi-natural grasslands on Öland – a preliminary study.
127. Karlberg, H., (2006): Vegetationsinventering med rumsligt högupplösande satellitdata – en studie av QuickBirddata för kartläggning av gräsmark och konnektivitet i landskapet.
128 Malmgren, A., (2006): Stormskador. En fjärranalytisk studie av stormen Gudruns skogsskador och dess orsaker.
129 Olofsson, J., (2006): Effects of human land-use on the global carbon cycle during the last 6000 years.
130 Johansson , T., (2006): Uppskattning av nettoprimärproduktionen (NPP) i stormfällen efter stormen Gudrun med hjälp av satellitdata.
131 Eckeskog, M., (2006): Spatial distribution of hydraulic conductivity in the Rio Sucio drainage basin, Nicaragua.
132 Lagerstedt, J., (2006): The effects of managed ruminants grazing on the global carbon cycle and greenhouse gas forcing.
133 Persson, P., (2007): Investigating the Impact of Ground Reflectance on Satellite Estimates of Forest Leaf Area Index
134 Valoczi, P. (2007): Koldioxidbalans och koldioxidinnehållsimulering av barrskog I Kristianstads län, samt klimatförändringens inverkan på skogen.
135 Johansson, H. (2007): Dalby Söderskog - en studie av trädarternas

sammansättning 1921 jämfört med 2005

137 Kalén, V. (2007): Analysing temporal and spatial variations in DOC concentrations in Scanian lakes and streams, using GIS and Remote Sensing

138 Maichel, V. (2007): Kvalitetsbedömning av kväveretentionen i nyanlagda våtmarker i Skåne

139 Agardh, M. (2007): Koldioxidbudget för Högestad – utsläpp/upptag och åtgärdsförslag

140 Peterz, S. (2007): Do landscape properties influence the migration of Ospreys?

141 Hendrikson, K. (2007): Småvatten och groddjur i Täby kommun

142 Carlsson, A. (2008): Antropogen påverkan i Sahel – påverkar människans aktivitet NDVI uppmätt med satellit.

143 Paulsson, R. (2008): Analysing climate effect of agriculture and forestry in southern Sweden at Högestad & Christinehof Estate

144 Ahlstrom, A. (2008): Accessibility, Poverty and Land Cover in Hambantota District, Sri Lanka. Incorporating local knowledge into a GIS based accessibility model.

145 Svensson T. (2008): Increasing ground temperatures at Abisko in Subarctic Sweden 1956-2006

146 af Wåhlberg, O. (2008): Tillämpning av GIS inom planering och naturvård - En metodstudie i Malmö kommun.

147 Eriksson, E. och Mattisson, K. (2008): Metod för vindkraftslokalisering med hjälp av GIS och oskarp logik.

148 Thorstensson, Helen (2008): Effekterna av ett varmare klimat på fenologin hos växter och djur i Europa sedan 1950.

149 Raguz, Veronika (2008): Karst and Waters in it – A Literature Study on Karst in General and on Problems and Possibilities of Water Management in Karst in Particular.

150 Karlsson, Peggy (2008): Klimatförändringarnas inverkan på de svenska vägarna.

151 Lyshede, Bjarne Munk (2008): Rapeseed Biodiesel and Climate Change Mitigation in the EU.

152 Sandell, Johan (2008): Detecting land cover change in Hambantota district, Sri Lanka, using remote sensing & GIS.

153 Elgh Dalgren, Sanna (2008): vattennivåförändringar i Vänern och dess inverkan på samhällsbyggnaden I utsatta städer

154 Karlgård, Julia (2008): Degrading palsa mires i northern Europe: changing vegetation in an altering climate and its potential impact on greenhouse gas fluxes.

155 Dubber, Wilhelm and Hedbom, Mari (2008) Soil erosion in northern Loa PDR – An evaluation of the RUSLE erosion model

156 Cederlund, Emma (2009): Metodgranskning av Klimatkommunernas lathund för inventering av växthusgasutsläpp från en kommun

157 Öberg, Anna (2009): GIS-användning i katastrofdrabbade utvecklingsländer